

Free radical generation by cultured mouse skeletal muscle cells

David M. Pattwell, Anne McArdle and Malcolm J. Jackson

Department of Medicine, University of Liverpool, Liverpool L69 3GA, UK

It has been extensively reported that free radical species are generated by contracting skeletal muscle following different exercise protocols (O'Neill *et al.* 1996; Reznick *et al.* 1996; McArdle *et al.* 2001), including non-damaging contractions (McArdle *et al.* 2001). However, numerous non-muscle cells are found in skeletal muscle *in vivo* and the presence of these cells has complicated the interpretation of these data.

Previous studies have shown that skeletal muscle cell cultures, which were electrically stimulated to contract, are a major source of superoxide radicals (McArdle *et al.* 2001). However, the site of production of these species remains unresolved. Production of superoxide release has been postulated to be from a number of sources (O'Neill *et al.* 1996; McArdle *et al.* 2001).

The aim of this study was to determine whether free radical species are generated in stimulated skeletal muscle myotubes in response to non-damaging contractions and to examine the possible source of this increased production of free radicals. H_2K -derived mouse myotubes (Harris *et al.* 1999) were electrically stimulated to contract in culture for 15 min (50 Hz frequency with pulses of 2 ms duration and 30 V $well^{-1}$) using platinum electrodes. The generation of hydroxyl and superoxide radicals was determined as previously described (McArdle *et al.* 2001; Pattwell *et al.* 2001). Data were analysed with Student's unpaired *t* test, $n = 12$, and data are presented as means \pm S.E.M.

Data indicate that 15 min of stimulation resulted in significant increases ($P < 0.05$) in superoxide (36 ± 6 cf. control 1 ± 0.01 nmol $(15 \text{ min})^{-1}$) and hydroxyl (0.60 ± 0.09 cf. 0.04 ± 0.01 nmol $(15 \text{ min})^{-1}$) radical production. Stimulation of the myotubes in the presence of the nitric oxide inhibitor, L-NAME, resulted in a further increase in superoxide production (45 ± 7 nmol $(15 \text{ min})^{-1}$, $P < 0.05$). Superoxide production was significantly decreased ($P < 0.05$) by cells that were stimulated to contract in the presence of diphenyleneiodium (DPI), an NADPH oxidase inhibitor or in the presence of superoxide dismutase (SOD) (DPI: 19.7 ± 4.3 nmol $(15 \text{ min})^{-1}$; SOD: 24 ± 6.7 nmol $(15 \text{ min})^{-1}$), respectively. These data indicate that free radical species are released by skeletal muscle cells during contraction and indicate possible sites of production of these radical species.

Harris, J.M. *et al.* (1999). *Exp. Cell Res.* **253**, 523–532.

McArdle, A. *et al.* (2001). *Am. J. Physiol.* **280**, C621–627.

O'Neill, C.A. *et al.* (1996). *J. Appl. Physiol.* **81**, 1197–1206.

Pattwell, D.M. *et al.* (2001). *FRBM* **30**, 979–985.

Reznick, A.Z., Packer, L., Sen, C.K., Holloszy, J.O. & Jackson, M.J. (eds) (1996). *Oxidative Stress in Skeletal Muscle*. Birkhauser Verlag.

H_2K cells were a kind gift from Professor T.A. Partridge and Dr J. Morgan, Imperial School of Medicine, Hammersmith Hospital, London, UK. This work was supported by The Wellcome Trust.

Catecholamine-induced myocyte necrosis in cardiac and skeletal muscles of the rat

D. Goldspink*, J. Burniston*, H. Cox*, W. Clark†, J. Colyer‡ and L.-B. Tan§

*Research Institute for Sports and Exercise Sciences, John Moores University, Liverpool, UK, †Michael Reese Medical Center, Chicago, USA and Departments of ‡Biochemistry and Molecular Biology and §Medicine, University of Leeds, Leeds, UK

In chronic heart failure continuous activation of the sympathetic system leads to sustained high levels of circulating catecholamines (Anker *et al.* 1997). These hormones can cause cardiomyocyte death, thereby contributing to further progressive cardiac dysfunction. Although it is possible that similar catecholamine-induced injury may be manifest in skeletal muscles, to date this has been inadequately studied despite substantial losses in muscle mass in some patients. We have used an animal model in which myocyte-specific necrosis can be detected and quantified in cardiac and skeletal muscles of the rat in response to a single injection (s.c.) of the synthetic catecholamine, isoprenaline. Male Wistar rats (*Rattus norvegicus*) weighing 301 ± 4.1 g were used, with all experimental procedures carried out under the UK Animals (Scientific Procedures) Act, 1986. Rats were administered (i.p.) an anti-myosin antibody at 1 mg kg^{-1} 1 h before the single injection of isoprenaline, which ranged in dose from 0.0001 to 5 mg kg^{-1} . Myocyte necrosis *in vivo* can be studied in this way as the antibody is excluded from normal cells, but is admitted through the disrupted sarcolemmal membranes of necrotic myocytes. Rats were killed by cervical dislocation at either 12 h for the soleus muscle or 18 h for the heart. Muscles were quickly isolated and snap frozen. Necrotic myocytes were visualised on $5 \mu\text{m}$ cryo-sections using secondary immunoperoxidase with 3,3'-diaminobenzidine (DAB). Image analysis was used to measure both the number (soleus) and area (ventricular subendocardium) of necrotic myocytes in randomly selected fields of view. Both muscle types were damaged by the isoprenaline, but with this occurring at lower doses in the skeletal muscle (Fig. 1).

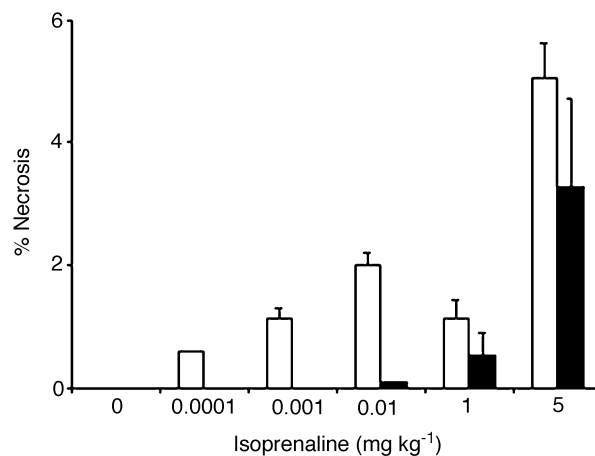


Figure 1. Dose dependency of isoprenaline-induced necrosis *in vivo* for soleus (□) at 12 h and subendocardium (■) at 18 h. All data are means \pm S.E.M. ($n = 3$ –8).

Peak myocyte necrosis also occurred earlier (12 h) in the soleus, compared with the heart (18 h). Although damaging both types of myocytes through β -adrenergic (AR) pathways, this catecholamine acted via different receptor subtypes, i.e. β_1 -ARs in the heart and β_2 -ARs in the soleus. Clearly skeletal muscle, as well as the heart, can be severely damaged by elevated catecholamines. Indeed, the skeletal myocytes appear to be more sensitive than

cardiomyocytes to the myotoxic effects. Although not a model of heart failure, our data support the concept of elevated catecholamines inducing a generalised, rather than cardiac-specific, myopathic process in heart failure (Opasich *et al.* 1999).

Anker, S.D. *et al.* (1997). *Circulation* **96**, 526–534.

Opasich, C. *et al.* (1999). *Eur Heart J.* **20**, 1191–1200.

The research was supported by the BHF and NHRF.

All procedures accord with current UK legislation.

The synthetic catecholamine, isoprenaline, induces apoptosis and necrosis in the soleus muscle of the rat

G. Ellison*, H. Cox*, D. Goldspink*, J. Burniston*, W. Clark†, and L.-B. Tan‡

*Research Institute for Sports and Exercise Sciences, John Moores University, Liverpool, UK, †Michael Reese Medical Center, Chicago, USA and ‡Department of Medicine, University of Leeds, Leeds, UK

Higher than normal levels of catecholamines are found in heart failure patients (Anker *et al.* 1997) and may, through a process of myocyte death, be involved in a progressive functional deterioration of the skeletal musculature as well as the heart. In our studies using a rat model, we have observed both myocyte necrosis and apoptosis in the soleus muscle after administering the synthetic catecholamine, isoprenaline, in the form of a single injection. Male Wistar rats (*Rattus norvegicus*) weighing 302.6 ± 3.4 g were used, with all experimental procedures carried out under the UK Animals (Scientific Procedures) Act, 1986. Fibre damage via necrosis was detected *in vivo* using an anti-myosin monoclonal antibody that only permeates the disrupted sarcolemmal membranes of necrotic fibres. All animals were injected i.p. with 1 mg kg⁻¹ of the myosin antibody 1 h before s.c. administration of various doses (ranging from 0.0001 to 5.0 mg kg⁻¹) of isoprenaline. Twelve hours later, rats were killed by cervical dislocation and the soleus muscles quickly isolated and snap frozen. The myosin antibody and an antibody directed against caspase 3 (R and D Systems), an enzyme that is activated during apoptosis, were detected on 5 µm cryo-sections using immunofluorescence. Fluorescein anti-mouse conjugated secondary antibody and Texas red anti-rabbit conjugated secondary antibody (Vector Labs) were used to visualise necrosis and apoptosis, respectively. The number of fibres damaged was counted in at least three random fields (~500 fibres) using image analysis and the results (Fig. 1) expressed as the percentage of the total number of fibres.

A one way ANOVA was employed to analyse the data for necrosis and Tukey's *post-hoc* analysis was used to locate the differences. For apoptosis, a Kruskal-Wallis test was employed, followed by Mann-Whitney *U* tests to locate the differences. No cell death was detected in control animals which received the saline vehicle only. In contrast, both myocyte necrosis and apoptosis were detected after administering 0.0001 mg of isoprenaline kg⁻¹ each reaching a maximum after 5 mg kg⁻¹ (Fig. 1). Roughly similar amounts of death occurred through both processes with some co-localisation between apoptotic and necrotic fibres being observed.

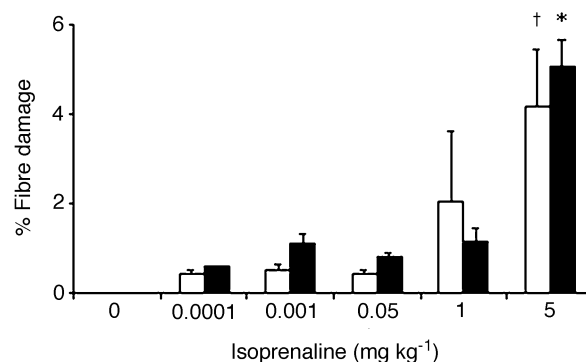


Figure 1. Necrosis (■) or apoptosis (□) in response to varying doses of isoprenaline *in vivo* in the soleus muscle. All data are means \pm S.E.M. ($n = 3$ –8). *Significant difference ($P < 0.05$) between 5 mg kg⁻¹ isoprenaline and all other doses. †Significant difference ($P < 0.01$) between 5 mg isoprenaline kg⁻¹ and 0.

Catecholamine-induced damage in skeletal muscle appears to involve both apoptosis and necrosis. Whether these represent two independent processes or not, and consequently the ability of satellite cells to regenerate these severely injured fibres, will be discussed.

Anker, S.D. *et al.* (1997). *Circulation* **96**, 526–534.

The research was supported by the BHF and NHRF.

All procedures accord with current UK legislation.

Mechanisms responsible for attenuated adaptive responses in skeletal muscle of aged mice following contractile activity

Aphrodite Vasilaki, Lesley Iwanejko, Francis McArdle, Malcolm J. Jackson and Anne McArdle

Departments of Medicine and Biological Sciences, University of Liverpool, Liverpool L69 3GA, UK

Skeletal muscle generates a number of free radical species during contraction. Muscles have developed adaptive mechanisms to protect against this increased production of free radicals by the up-regulation of antioxidant enzymes (including catalase and superoxide dismutase (SOD)) and heat shock proteins (HSPs) (McArdle *et al.* 2002). We have demonstrated that the ability of muscles of aged rodents to adapt following contractile activity is severely attenuated (Vasilaki *et al.* 2002), although the mechanisms responsible for this attenuation have not been established.

The aim of this study was to characterise the extent and time course of production of antioxidant enzymes and HSPs in muscles of adult and aged mice following a severe contraction protocol and to examine the mechanisms responsible for attenuation of the stress response in skeletal muscle of aged mice following exercise.

Male adult (14–16 months old) and aged (29–32 months old) B6XSJL mice were anaesthetised with an i.p. injection of sodium pentobarbitone (65 mg (100 g body wt)⁻¹). Hindlimbs were subjected to a 15 min period of isometric contractions via surface electrodes. Mice were killed humanely by an overdose of anaesthetic at different time points following the contraction

protocol and anterior tibialis muscles were analysed for activity of catalase and superoxide dismutase and HSP content at various time points (McArdle *et al.* 2001). Muscles were analysed for heat shock factor 1 (HSF1) and nuclear factor κ B (NF- κ B) DNA binding activity immediately following the contraction protocol (Mosser *et al.* 1988). Data were analysed with analysis of variance and modified Bonferonni's *t* test, $n = 5-6$. Data are presented as means \pm S.E.M.

The period of exercise resulted in a significant rise in catalase activity (non-exercised: 0.6 ± 0.2 U (mg protein) $^{-1}$, 12 h post-exercise: 2.4 ± 0.6 U (mg protein) $^{-1}$, $P < 0.05$) and SOD activity (non-exercised: 32.3 ± 5.4 U (mg protein) $^{-1}$, 12 h post-exercise: 49.7 ± 3.7 U (mg protein) $^{-1}$, $P < 0.05$) in muscles of adult mice. In addition, the HSC70 content of muscles from adult mice was significantly increased following the exercise protocol (e.g. 4 h post-exercise: adult mice: $144.4 \pm 8.4\%$ of non-exercised control, $P < 0.05$). This response was not evident in muscles of aged mice. In muscles of aged mice, binding of HSF1 to the heat shock element (HSE) binding domain was not grossly altered. However, the binding of NF- κ B from muscles of old mice to the NF- κ B binding domain was severely attenuated.

These data suggest that the inability of muscles of aged mice to produce HSPs following contractile activity may not be due to an altered binding of HSF1 to the HSE. In contrast, this may be the mechanism by which production of antioxidant enzymes is altered in aged mice following exercise.

McArdle, A. *et al.* (2001). *Am. J. Physiol. Cell. Physiol.* **280**, C621–627.

McArdle, A. *et al.* (2002). *Ageing Res. Rev.* **1**, 79–93.

Mosser, D.D. *et al.* (1988). *Mol. Cell Biol.* **8**, 4736–4744.

Vasilaki, A. *et al.* (2002). *Muscle and Nerve* **25**, 902–905.

The authors would like to thank the University of Liverpool and Research into Ageing for financial support.

All procedures accord with current UK legislation.

Lifelong over-expression of HSP70 in skeletal muscle of transgenic mice protects against age-related functional deficits

A. McArdle*, C.S. Broome*, W. Dillmann†, R. Mestrliz‡, J.A. Faulkner§ and M.J. Jackson*

*University of Liverpool, Liverpool, UK, †University of California, San Diego, USA, ‡Loyola University, Chicago, USA and §University of Michigan, USA

Skeletal muscle of young rodents responds to a demanding contraction protocol by an increased production of stress or heat shock proteins (HSPs; McArdle *et al.* 2001). Skeletal muscles of ageing rodents are characterised by a severe attenuation of this ability to produce HSPs in response to a demanding contraction protocol (Vasilaki *et al.* 2002). The functional effect of this attenuated response is not known. This study has used transgenic mice to examine the role that this attenuated stress response plays in the susceptibility of muscles to contraction-induced injury and the nature of recovery following this injury.

Mice were anaesthetised by i.p. injection of sodium pentobarbitone (65 mg (100 g body wt) $^{-1}$). Extensor digitorum longus muscles of adult (12–14 months) and old (26–30 months) wild-type and transgenic mice, over-expressing HSP70 (Marber *et al.* 1995), were subjected to damaging lengthening contractions (3×5 min periods of contractions, with 5 min intervals, during which the muscle was activated at 150 Hz and

lengthened by 20% of fibre length every 2 s). At 3 h, and 3, 14 and 28 days following the contraction protocol, mice were anaesthetised and the recovery of muscles was measured by the ability to generate maximum force. Mice were humanely killed by overdose of sodium pentobarbitone. Muscle structure, biochemical and immunohistochemical markers of muscle damage and regeneration were assessed. Data are presented as means \pm S.E.M. Data are analysed using ANOVA with a modified Bonferonni test, $n = 4-8$.

A similar fall in the force generation was seen in muscles of adult and old wild-type and HSP70 transgenic mice at 3 h following the contraction protocol (adult wild-type: 37 ± 6 , adult HSP70: 38 ± 10 , old wild-type: 42 ± 7 , old HSP70: $29 \pm 3\%$ of pre-exercise value). However, muscles of adult and old wild-type mice demonstrated a further loss of force generation at 3 days following the contraction protocol (adult: $24 \pm 7\%$, old: $27 \pm 7\%$ of pre-exercise values), which was significantly ($P < 0.05$) lower than the value at 3 h following the contraction protocol. There was no evidence of a secondary loss of force in muscles of adult or aged HSP70 transgenic mice at this time point (adult: 37 ± 4 , old: 38 ± 14). The maximum force generated by muscles of adult transgenic mice had recovered to pre-exercise values by 14 days following the contractions, whereas a significant ($P < 0.05$) deficit remained in the muscles of adult wild-type mice (HSP70: $85 \pm 15\%$, wild-type: $46 \pm 10\%$ of pre-exercise value, $P < 0.05$). Muscles of adult wild-type mice had recovered to pre-exercise values by 28 days following the contraction protocol. The ability of muscles from old transgenic mice to recover following damage was maintained, whereas a significant ($P < 0.05$) deficit existed in muscles of old wild-type mice at 28 days following the contractile protocol ($56 \pm 7\%$ of pre-exercise value).

These data indicate that the diminished production of HSP70 in muscles of old mammals has a major effect on age-related functional deficits in muscle.

McArdle, A. *et al.* (2001). *Am. J. Physiol. Cell. Physiol.* **280**, C621–627.

Marber, M.S. *et al.* (1995). *J. Clin. Invest.* **95**, 1446–1456.

Vasilaki, A. *et al.* (2002). *Muscle and Nerve* **25**, 902–905.

The authors would like to thank Research into Ageing for funding this work.

All procedures accord with current UK legislation.

Activation properties of quadriceps muscles in patients with nemaline myopathy

H.L. Gerrits*, I.M.G. Gommans*,†, B.G.M. van Engelen† and A. de Haan*

*Institute for Fundamental and Clinical Human Movement Sciences, *Vrije Universiteit, Amsterdam, The Netherlands and †University Medical Center, St Radboud, Nijmegen, The Netherlands*

Nemaline myopathy is a congenital neuromuscular disorder, characterised by severe muscle weakness, predominantly of proximal limb muscles (Wallgren-Pettersson *et al.* 1999), which seems not directly linked to muscle atrophy. The nature of this muscle weakness is presently unclear but may be related to peripheral as well as central aspects of neuromuscular control. This study seeks to improve the understanding of underlying processes that may be responsible for the muscle weakness found in these patients. The aim of the present study was to investigate whether voluntary activation and/or activation frequency contribute to the weakness experienced in the quadriceps muscle.

The local ethical committee approved this study. Voluntary isometric knee extension torque (MVC) was obtained at 60 deg knee flexion angle in ten patients of one family with nemaline myopathy and eight healthy controls (4 from the same family). A superimposed stimulation technique (supramaximal triplet at 300 Hz applied via surface electrodes) was used to assess the degree of voluntary activation and electrically evoked twitch and tetanic (10, 20, 50, 150 Hz) torque responses were obtained. Further, MVC (with superimposed stimulation) was measured at different angles of knee flexion (30, 40, 50, 60 and 70 deg).

At 60 deg voluntary torque was significantly lower (Student's unpaired *t* test; $P < 0.05$) in patients (mean \pm S.E.M.; 125 ± 10 Nm) compared with controls (194 ± 20 Nm). This was not due to an impairment of voluntary activation, since activation was even higher ($P < 0.05$) in the patient group (95 vs. 85 %). The patients showed greater relative torques at low stimulation frequencies ($P < 0.05$). For example, with 10 Hz stimulation relative torques were 51 ± 5 and 25 ± 3 % in patients and controls, respectively. Maximal voluntary torque was found, as expected, at ~ 60 deg knee flexion in the controls but at a significantly lower ($P < 0.05$) angle in the patient group (~ 45 deg).

In conclusion, nemaline myopathy seems to lead to changes at the peripheral site of neuromuscular performance, as indicated by the higher relative forces observed for the patients at low frequencies of activation. However, this finding is probably not directly related to the disease but can be attributed to adaptations in muscle morphology in the patients, i.e. the observed shift in the knee angle–torque relationship and the reported relatively large proportion of type I fibres (Gommans *et al.* 2002).

Gommans, I.M.G. *et al.* (2002). *Neuromusc. Disord.* **12**, 13–18.

Wallgren-Pettersson, C. *et al.* (1999). *Neuromusc. Disord.* **9**, 564–572.

All procedures accord with current local guidelines and the Declaration of Helsinki.

Intracellular and mitochondrial Ca^{2+} in mouse intact soleus skeletal muscle fibres during repeated intermittent tetanic stimulation

J.D. Bruton, H. Westerblad and J. Lännergren

Department of Physiology & Pharmacology, Karolinska Institute, S-171 77 Stockholm, Sweden

In frog skeletal muscle fibres subjected to repeated intermittent tetanic contractions, force production decreases due to reduced tetanic Ca^{2+} transients. Relaxation of force also slows due to slowed Ca^{2+} uptake into the sarcoplasmic reticulum (SR). Repeated tetanic stimulation also causes mitochondrial Ca^{2+} to increase, which may be detrimental to muscle performance. We were interested to determine if muscle fibres from a slow-twitch mammalian muscle showed similar changes during a bout of repetitive activity.

Adult NMRI mice were killed by cervical dislocation. Intact single fibres were mechanically dissected from the soleus muscles. Clips were attached to the tendons. One clip was attached to a force transducer and the other to an adjustable holder. The fibre length was set to the length giving maximum tetanic force. A total of 21 fibres was used in these experiments. In seven fibres, free myoplasmic Ca^{2+} ($[\text{Ca}^{2+}]_i$) was measured using the fluorescent indicator, Indo-1. In the remaining 13 fibres, the free Ca^{2+} in the mitochondrial matrix was monitored using changes in the Rhod-2 fluorescent signal (expressed in arbitrary units, a.u.). Fibres were stimulated repeatedly with

70 Hz, 500 ms tetani at 2 s intervals for 1000 tetani or until force fell to 40 % of its initial value. All values shown are means \pm S.E.M. Significance was tested with Student's *t* test.

Tetanic $[\text{Ca}^{2+}]_i$ rose from $1.74 \pm 0.26 \mu\text{M}$ in the first tetanus to $3.10 \pm 0.87 \mu\text{M}$ ($n = 7$) in the tenth tetanus, while force fell to 93.5 ± 2.3 % ($n = 7$) of the starting value. Thereafter, tetanic $[\text{Ca}^{2+}]_i$ fell slightly and in the last tetanus of the series was $1.91 \pm 0.50 \mu\text{M}$ ($n = 27$) and not significantly higher than control. Tetanic force also decreased slightly and was significantly reduced from control ($P < 0.05$) to 74 ± 6 % ($n = 6$) in the final tetanus. There was no evidence of any slowing of Ca^{2+} uptake into the SR as basal $[\text{Ca}^{2+}]_i$ was 71.2 ± 14.6 nM ($n = 7$) and 89.2 ± 15.8 nM ($n = 7$) prior to the first and last tetanus of the series, respectively.

In the 14 fibres loaded with Rhod-2 and stimulated as described above, 10 fibres showed a marked increase in the Rhod-2 signal (indicating that mitochondrial Ca^{2+} had increased) while the remaining four showed no change. In those fibres in which mitochondrial Ca^{2+} increased, a peak Rhod-2 signal of 9.1 ± 1.7 a.u. ($n = 9$) occurred within 50 tetani. Thereafter, the Rhod-2 signal fell slowly to about half of this peak value by the time stimulation was stopped. Interestingly, there was a significant inverse correlation between the amplitude of the Rhod-2 signal at the end of stimulation and the extent of force depression. Thus mitochondrial Ca^{2+} accumulation does not impair force production.

All procedures accord with current National guidelines.

Stretch-induced increase in myoplasmic calcium in resting neonatal rat muscle fibres

G. Mutungi* and K.A.P. Edman†

**Department of Physiology, University of Bristol, Bristol BS8 1TD, UK and †Department of Physiological Sciences, BMC, F11, University of Lund, S-221 84 Lund, Sweden*

Recent experiments have shown that a large triangular length change (> 20 % of initial muscle length, L_o) applied to a small resting muscle fibre bundle isolated from 7-day-old rats has two specific effects on passive tension (Mutungi & Ranatunga, 2001a,b). Thus in addition to the transitory passive tension response that accompanies the stretch, a twitch-like tension appears immediately after the stretch-release cycle. The latter is 30–50 % of the isometric twitch tension, and is only seen in neonatal rat muscle fibres. Except for results, such as the effects of BDM and dependence on sarcomere length (Mutungi & Ranatunga, 2001b) that suggest that the twitch-like response may be based on cross-bridge activity, the mechanisms underlying this phenomenon still remain unclear. The present experiments were aimed at investigating whether the twitch-like response to stretch is associated with intracellular calcium release.

The experiments were performed at 20 °C using small muscle fibre bundles (~ 10 – 15 muscle fibres) isolated from neonatal rats killed using carbon dioxide. Both soleus and extensor digitorum longus (edl) twitch muscles were used. Preparations were mounted horizontally between two stainless-steel hooks, one attached to a servomotor and the other to a tension transducer in a muscle chamber. After the initial length was set for optimum twitch tension, the preparation was subjected to a rapid stretch-release cycle (amplitude ~ 25 % L_o) and the tension and intracellular calcium levels monitored. The level of intracellular calcium was monitored using Fluo-3 AM following the procedure described by Caputo *et al.* (1994).

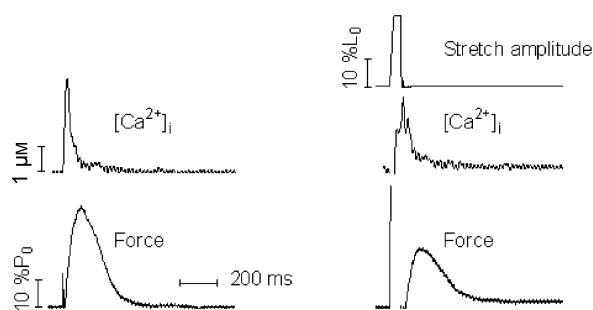


Figure 1. Effects of a stretch-release cycle on force and intracellular calcium concentration. The traces are from an edl fibre bundle isolated from a 5-day-old rat. Left panel: isometric twitch. Right panel: passive stretch-release movement. Note that the length change is followed by a pronounced increase in both tension and intracellular calcium.

As Fig. 1 shows, the stretch phase was immediately followed by an increase in intracellular calcium and, after the completed stretch-release cycle, by a twitch-like tension response. Moreover, the amplitude of the stretch-induced myoplasmic calcium transient was smaller than that recorded during the control isometric twitch. Similar observations were made in all seven preparations (4 edl and 3 soleus) studied. These results demonstrate that a rapid stretch of muscle fibre bundles isolated from neonatal rats leads to an increase in intracellular calcium that causes activation of the contractile system.

Caputo, C. *et al.* (1994). *J. Physiol.* **478**, 137–148.

Mutungi, G. & Ranatunga, K.W. (2001a). *J. Physiol.* **536.P**, 7P.

Mutungi, G. & Ranatunga, K.W. (2001b). *J. Physiol.* **536.P**, 88P.

This work was supported by grants from The Wellcome Trust and the Swedish Medical Research Council.

All procedures accord with current local guidelines and the Declaration of Helsinki.

The influence of mode of muscle contraction on muscle blood flow in man

D. Ball, G. Fordy, E. Dawson and K.P. George

Centre for Biophysical and Clinical Research into Human Movement, Manchester Metropolitan University, Alsager ST7 2HL, UK

Muscle blood flow is influenced by the metabolic demands placed upon the exercising musculature. Since the metabolic cost of eccentric exercise is lower than that of concentric exercise (Woledge *et al.* 1985), at an equivalent degree of force/power production, it has been suggested that the blood flow would be concomitantly lower (Nadel *et al.* 1972). Whether this difference in blood flow exists has not to our knowledge been tested. The aim of the present investigation was to measure blood flow during 6 min of single leg knee-extensor exercise when the mode of contraction was concentric on one occasion and eccentric on another.

With ethics committee approval seven healthy subjects (6 males and 1 female) volunteered for the present study. Their physical characteristics were (mean \pm s.d.) age 26 ± 4 years, mass 80.1 ± 7.9 kg and height 1.78 ± 0.05 m. Subjects completed two exercise trials on an isokinetic dynamometer (Lido, Loredan

Biomedical Inc., Davis, CA, USA) where the mode of contraction was either concentric (CON) or eccentric (ECC) in nature. Total exercise duration was 6 min, consisting of four 90 s bouts interspersed with 15 s of rest. Exercise mode was completed in randomised order and the trials were separated by 70 min of passive rest. Femoral artery diameter and blood velocity was measured by ultrasound Doppler (Esaote Biomedica AU4 Idea) at an imaging frequency of 10 MHz. Blood velocity was measured at rest and immediately after each exercise bout. Pulmonary oxygen uptake was measured continuously through exercise using an Oxycon Alpha (Erich Jaeger B.V., The Netherlands). Data were analysed using two-way ANOVA with repeated measures and *post-hoc* Tukey test, and where appropriate Student's paired *t* test.

The total work done on the muscle was greater ($P < 0.01$) during the eccentric mode of exercise compared with total work done by the muscle during the concentric mode (30.70 ± 8.37 vs. 20.04 ± 4.24 kJ). However, the metabolic cost of exercise, as estimated from net oxygen consumption, was higher ($P < 0.05$) during CON compared with ECC (52.6 ± 23.4 vs. 41.7 ± 23.4 l). Blood flow at rest was similar between conditions (CON, 1.00 ± 0.28 l min⁻¹; ECC 1.05 ± 0.18 l min⁻¹). Throughout each exercise trial blood flow was higher ($P < 0.01$) during CON than ECC, so that the average blood flow was 2.96 ± 0.95 l min⁻¹ during CON and 1.92 ± 1.02 l min⁻¹ during ECC.

The results of the present study confirm the suggestion that blood flow during eccentric mode contractions is lower than concentric contractions. The fact that during eccentric exercise work is done *on* the muscle rather than work *by* the muscle is reflected by the lower oxygen cost of eccentric exercise that would result in a reduced metabolic drive to increase blood flow.

Nadel, E.R. *et al.* (1972). *J. Appl. Physiol.* **33**, 553–558.

Woledge, R.C., Curtin, N.A. & Homsher, E. (1985). *Energetic Aspects of Muscle Contraction*, pp. 201–217. Academic Press.

All procedures accord with the Declaration of Helsinki.

Influence of long-term bed rest on muscle architecture and tendon mechanical properties

N. Reeves*, C.N. Maganaris*, G. Ferretti† and M.V. Narici*

*Centre for Biophysical and Clinical Research into Human Movement, Manchester Metropolitan University, Alsager Campus, UK and †Centre Médical Universitaire, University of Geneva, Switzerland

Muscle weakness and atrophy are well-known consequences of microgravity exposure. However, little is known about how this condition affects the internal structure of the muscle, properties of the tendons and their functional consequences. Therefore, to simulate the effects of microgravity, six males (age 32.7 ± 3.6 years; height 1.73 ± 0.04 m; body mass 71.5 ± 6.3 kg, means \pm s.d.) underwent a period of long-term bed rest (LTBR) lasting 90 days. This study (LTBR-2001) was organised by ESA together with NASDA and CNES and performed in Toulouse, France. Ethical committee approval was gained from the host institution.

Gastrocnemius medialis (GM) muscle architecture (GM cross-sectional area, fibre fascicle length and pennation angle) and tendon dimensions and mechanical properties were studied *in vivo* using real-time ultrasonography and magnetic resonance imaging, before and after LTBR. Subjects were seated, the right

foot securely positioned in a dynamometer and the knee flexed at 90 deg. Changes in muscle architecture were assessed during graded isometric contraction at 40, 60 and 100 % of the maximal voluntary plantarflexion (MVP), at 20 deg of dorsiflexion. Changes in tendon stiffness were assessed during a MVP after normalisation for tendon dimensions (Young's module, i.e. stress/strain).

Paired-samples Student's *t* test was used to detect changes pre- to post-LTBR; level of significance was set at $P < 0.05$. After LTBR (1) plantarflexion force was reduced by $55 \pm 19\%$ ($P < 0.01$); (2) fascicle length and pennation angle were reduced by $9 \pm 3\%$ ($P < 0.01$) and $14 \pm 5\%$ ($P < 0.01$), respectively; (3) cross-sectional areas of the GM muscle at mid-calf level, were reduced by $32 \pm 2\%$ ($P < 0.001$), and (4) the GM tendon Young's modulus at MVP was reduced by $32 \pm 5\%$ ($P < 0.05$). These findings are in agreement with previous research in disuse conditions (Narici *et al.* 1998) and strongly suggest a loss of both in-series and in-parallel sarcomeres induced by the prolonged unloading during bed rest.

After LTBR percentage fascicle shortening during MVP was reduced by 35 ± 18 ($P < 0.01$). This is probably due to a loss of sarcomeres in-series limiting the extent of absolute fascicle shortening. Hence after LTBR, the same tendon force can be developed by a reduced fascicle shortening; this may be advantageous to remain on the same portion of the sarcomere length-tension relationship. Therefore the muscle atrophy associated with prolonged disuse involves significant changes in muscle architecture and of tendon mechanical properties. These structural and mechanical alterations are likely to have an effect on the length-force relationship of this muscle group and on its rate of force development.

Narici, M.V. *et al.* (1998). *J. Physiol.* **506.P**, 59P.

The Authors are grateful to Dr A. Maillet and to all the staff of MEDES for their superb support.

All procedures accord with current local guidelines and the Declaration of Helsinki.

Myo-muscular interactions: evidence for reciprocal inhibition between classes of muscle fibre

Andrew Packard

Stazione Zoologica 'A. Dohrn', Napoli, Italy

Figure 1 traces the changes in tension developed by muscle fibres – here classed as 'catch' type and 'tonic/phasic' – on the pigment spots of four overlapping populations of chromatophores in the skin of an intact squid (*Loligo vulgaris*). Polygonal profiles, due to catch type fibres, develop post-mortem as the motor nerves begin to die. They relax on stimulation with a brief seawater pulse and are replaced by round 'tonic/phasic' profiles. Expansion of the latter – signalling muscle contraction (or contracture) – are not directly induced by the original disturbance but by a clearing of the wave space left by relaxation (catch release) of the former. The two contractile states relate reciprocally to each other both within a single chromatophore (trace A), the muscle fibres of which are known to be coupled, and between classes (A/B and C/D). Time courses (10–20 s) for catch release and subsequent invasion of the wave space by tonic/phasic profiles vary with context. Cycling between the two continues post-mortem for many hours.

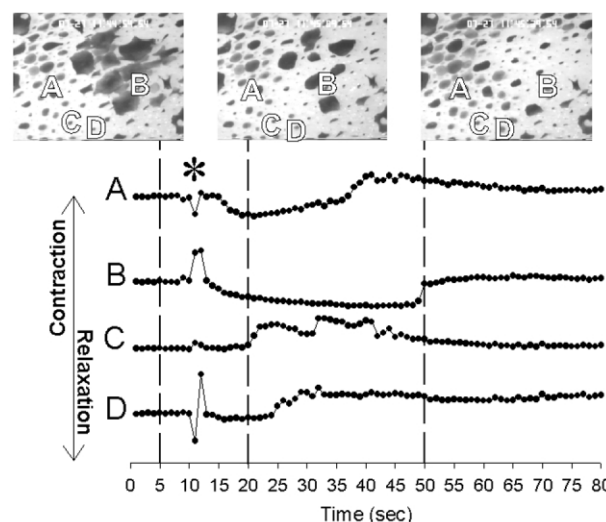


Figure 1. Muscle tension-dependent changes in profile of several chromatophore classes in dorsal mantle of a squid (video-frames) following disturbance by brief seawater pulse (*). Relaxation of 'catch' type muscle (A and B) induces phasic/tonic contractions in neighbouring spots (C and D).

In life they also have reciprocal roles. Spots expanded by catch type muscle are for feature generation against a clear skin; round profiles due to tonic/phasic muscle are for tone matching and countershading, with feature generation usually suppressed.

Computing and graphics were by L. Caputi.

The myosin II working stroke in presence of ATP analogues

M. Capitanio*, W. Steffen† and J. Sleep†

*LENS, via Nello Carrara 1, 50019 Sesto F. no (Florence) and Department of Physiology, University of Florence, V. le Morgagni 68, Florence, Italy and †MRC, Muscle and Cell Motility Unit, King's College London, London SE1 1UL, UK

ATP drives the normal actomyosin cross-bridge cycle in which M.ADP.P_i binds to actin and undergoes a working stroke during the release of products and formation of the rigor state (A.M). In recent years optical tweezers have been used by several laboratories to measure this working stroke at the single molecule level. The consensus value is around 6 nm. Other ligands such as pyrophosphate (PP_i) and ADP, which do not go through a hydrolytic cycle and are not a source of energy, do however weaken the interaction between myosin and actin, although to a lesser extent than ATP. When myosin states such as M.ADP and M.PP_i bind to actin do they still perform a working stroke? In the experiments, an actin filament is suspended between two optically trapped polystyrene beads and stretched taut, forming a 'dumb-bell'. The dumb-bell is then positioned over a fixed bead carrying a low density of S1 molecules. The images of the trapped beads are projected onto quadrant detector photodiodes to record bead displacements. In the absence of interaction the position signal is the noise due to the Brownian motion of the dumb-bell controlled by the trap stiffness, whereas when the S1 attaches to the actin filament, the S1 stiffness comes into play and reduces the position noise. In this way it is possible to distinguish between bound and unbound states and to measure the S1 working stroke.

Experiments with ATP ($5 \mu\text{M}$) gave working strokes in the range 5–6 nm and interaction half-lives of about 40 ms. With ADP ($500 \mu\text{M}$) interactions were much more prolonged ($t_{1/2} \sim 1.4$ s) particularly when hexokinase (1 mg ml^{-1}) was used to eliminate ATP contamination. Our estimate of the working stroke was 0.05 ± 0.7 nm.

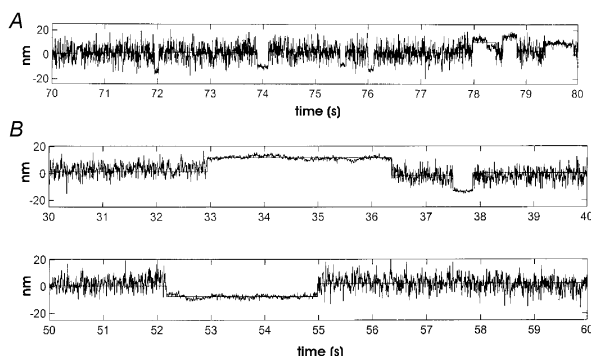


Figure 1. A, 10 s of the position record of a bead of the dumb-bell while interacting with S1 in the presence of PP_i ($100 \mu\text{M}$) and $[\text{KCl}] = 65 \text{ mM}$. B, 20 s of the position record of a bead of the dumb-bell while interacting with S1 in the presence of ADP ($500 \mu\text{M}$) and $[\text{KCl}] = 25 \text{ mM}$.

With PP_i we found that the rate of M.PP_i binding to actin was higher than with M.ADP.P_i and it was necessary to add 40 mM KCl to reduce this rate to allow the characterisation of single interactions. The length of interactions was dependent upon $[\text{PP}_i]$, the second-order binding constant being $10^5 \text{ M}^{-1} \text{ s}^{-1}$, which shows that during the interaction the A.M state must have been formed. The estimate of the working stroke was 0.2 ± 0.5 nm.

Temperature dependence of the axial motions of myosin heads during isometric contraction in single fibres from frog muscle

M. Reconditi*, G. Piazzesi*, M. Linari*, L. Lucii*, Y.-B. Sun†, P. Boesecke‡, T. Narayanan‡, V. Lombardi* and M. Irving†

*Department of Physiology, University of Florence, I-50134 Firenze, Italy, †School of Biomedical Sciences, King's College London, London SE1 1UL, UK and ‡ESRF, BP 220, 38043 Grenoble, France

Skeletal muscle fibres generally produce higher active isometric force at higher temperature. In intact fibres from frog skeletal muscle this is due to a higher force per myosin cross-bridge rather than an increase in the number of cross-bridges (Linari *et al.* 2001). We investigated the structural basis of the temperature effect by X-ray diffraction at beamline ID2 of the European Synchrotron Radiation Facility (ESRF), Grenoble, France, using single fibres from anterior tibialis muscle of frogs (*Rana temporaria*) that had been humanely killed. The sarcomere length was $2.1 \mu\text{m}$. Isometric tetanic force was $34 \pm 5\%$ (mean \pm S.D., $n = 5$ fibres) greater at 11°C than at 0°C . There was no change in the intensity of the first actin layer line, which is sensitive to the number of myosin heads attached to actin. The intensity of the M3 X-ray reflection from the axial repeat of the myosin heads along the filaments was $11 \pm 1\%$ (mean \pm S.D.) greater at the higher temperature. The fine structure of the M3 reflection, arising from interference between the two arrays of myosin heads in each myosin filament, was used to measure the axial position of the heads with respect to the centre of the filament (Linari *et al.* 2000). During an isometric tetanus the M3 reflection was composed of two well-resolved peaks. The ratio of

the intensity of the higher angle peak to that of the lower angle peak was 0.88 ± 0.10 at 0°C and 0.69 ± 0.09 at 11°C . This difference corresponds to an average shift of the centres of mass of the myosin heads towards the centre of the filament by 0.31 nm at the higher temperature. The changes in intensity and interference fine structure of the M3 reflection were analysed using a structural model for the myosin filament incorporating filament compliance and an atomic model for the myosin head in which force is generated by tilting of its light chain domain with respect to the catalytic domain (Rayment *et al.* 1993; Piazzesi *et al.* 2002). The results show that the observed increase in force per myosin head with increasing temperature can be explained by the tilting-light chain domain model.

Linari, M. *et al.* (2000). *Proc. Natl Acad. Sci. USA* **97**, 7226–7231.

Linari, M. *et al.* (2001). *Pflügers Arch.* **442**, R65.

Piazzesi, G. *et al.* (2002). *Nature* **415**, 659–662.

Rayment, I. *et al.* (1993). *Science* **261**, 58–65.

This work was supported by MRC (UK), MURST and Telethon (Italy), EU, EMBL and ESRF.

All procedures accord with current National guidelines.

Energetics of muscular exercise at work onset: the steady-state approach

P.E. di Prampero, M.P. Francescato and V. Cettolo

Department of Biomedical Sciences and Technologies, University of Udine, Italy

The aim of the present study was to show that it is possible to gain information on variables traditionally assessed during exercise transients from data obtained at steady state. A theoretical model is described, which shows that oxygen consumption above resting ($\Delta\dot{V}_{\text{O}_2}$), mechanical power (W) and phosphocreatine (PC) concentration at steady state are set by the time constant of the \dot{V}_{O_2} on response (τ), the O_2 equivalent of high energy phosphate splitting (c) and the mechanical work performed per unit of PC split (b). The model assumptions are as follows: (i) the muscle \dot{V}_{O_2} on response is monoexponential and (ii) it mirrors the fall of PC concentration (ΔPC), (iii) throughout the exercise lactic acid production is nil. If this is so: $\Delta\text{PC}/\Delta\dot{V}_{\text{O}_2} = c\tau$; $\Delta\dot{V}_{\text{O}_2}/W = (bc)^{-1}$ and $\Delta\text{PC}/W = \tau/b$. Thus in the three-dimensional space (c , b , τ) the experimental quantities $\Delta\text{PC}/\Delta\dot{V}_{\text{O}_2}$, $W/\Delta\dot{V}_{\text{O}_2}$ and $\Delta\text{PC}/W$ define a function where all triplets (c , b , τ) compatible with the experimental data must lie.

The range of c , τ and b was assessed on ten healthy volunteers performing rhythmic (0.83 Hz) dynamic exercise with the calf muscles of both legs (Francescato & Cettolo, 2001) inside the bore of a standard 1.5 T MR unit. W and $\Delta\dot{V}_{\text{O}_2}$ were measured at steady state and relative PC concentration (ΔPC) was simultaneously evaluated by ^{31}P -MR spectroscopy from the medial belly of the right gastrocnemius. $\Delta\dot{V}_{\text{O}_2}$ and W were expressed per unit of active muscle mass, as measured by MRI in separate experiments.

The relationships between $\Delta\dot{V}_{\text{O}_2}$ ($\text{mmol kg}^{-1} \text{ s}^{-1}$) and W (Watt kg^{-1}), between ΔPC and W and between ΔPC and $\Delta\dot{V}_{\text{O}_2}$ can be appropriately interpolated by straight line regressions, as described by: $\Delta\dot{V}_{\text{O}_2} = 5.23 \times 10^{-3} + 16.8 \times 10^{-3} W$ ($r = 0.952$), $\Delta\text{PC} = 0.0596 + 0.0625 W$ ($r = 0.861$) and $\Delta\text{PC} = 0.0412 + 3.71 \Delta\dot{V}_{\text{O}_2}$ ($r = 0.898$).

These data allowed us to calculate the inter-relationships among the three quantities c , τ and b ; they are represented

tridimensionally in Fig. 1 for the minimal and maximal PC concentrations to be expected in resting muscle (17.8 and 37.7 mmol kg⁻¹ fresh muscle; Rico-Sanz *et al.* 1999; Walter *et al.* 1999). Figure 1 shows that, for an O₂ equivalent of PC splitting (P/O₂ ratio) not far from 6, the mechanical equivalent of PC splitting is unaffected by resting PC concentration, amounting to about 10 J mmol⁻¹, whereas the time constant of the O₂ uptake at work onset increases with PC concentration from 10 to 25 s.

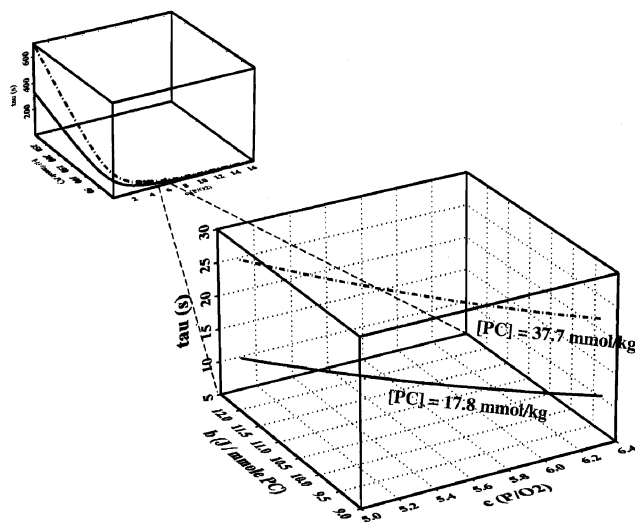


Figure 1. Tridimensional representation of the relationships among τ , c and b for the minimal and maximal PC concentrations reported in the literature (17.8 and 37.7 mmol kg⁻¹). The range over which c can be expected to vary is somewhat restricted, thus allowing us to obtain a set of reasonable solutions for the three quantities at stake.

These data support the view that the steady-state energetics are dependent on, and tightly coupled to, the events that occurred during the transient phase, of which the steady state can therefore be considered the 'memory'.

Francescato, M.P. & Cettolo, V. (2001). *MRM* **46**, 1000–1005.

Rico-Sanz, J. *et al.* (1999). *Med. Sci. Sports Exerc.* **31**, 1580–1586.

Walter, G. *et al.* (1999). *J. Appl. Physiol.* **519**, 901–910.

All procedures accord with current local guidelines.

Influence of relative muscle length on power production of rat medial gastrocnemius muscle

A. de Haan and M.R. van der Vliet

Institute for Fundamental and Clinical Human Movement Sciences, Vrije Universiteit, Van der Boechorststraat 9, 1081 BT Amsterdam, The Netherlands

It is generally assumed that the influence of relative muscle length as observed in isometric conditions is similar in dynamic (shortening) conditions, but there is little information available in the literature. The aim of the present study was to compare the influence of relative muscle length between isometric and dynamic contractions of maximally activated skeletal muscles. Medial gastrocnemius muscle–tendon complexes of anaesthetized (urethane 1.5 g (kg body mass)⁻¹; I.P.; $n = 18$) rats were stimulated via the severed sciatic nerve at 35°C. Stimulation frequencies used (250 Hz for isometric contractions and 400 Hz for shortening contractions) were high enough to maximally

activate the muscles at all relative muscle lengths. Force–velocity relations were obtained (de Haan, 1998) at four different muscle lengths: isometric optimum length (Lo_{iso}), $Lo_{iso} - 2$ mm, $Lo_{iso} - 4$ mm and $Lo_{iso} - 6$ mm. Length–force relations were measured at four different velocities: $v = 0, 50, 100$ and 150 mm s⁻¹. After the experiments the rats were humanely killed.

Average maximal isometric forces at relative lengths measured below Lo_{iso} were 96 % (at $Lo_{iso} - 2$ mm), 88 % (at $Lo_{iso} - 4$ mm) and 58 % (at $Lo_{iso} - 6$ mm) of the maximal isometric force at Lo_{iso} . Maximal rate of force rise was not different between Lo_{iso} and $Lo_{iso} - 2$ mm (~ 0.40 N s⁻¹) but lower at the lower lengths. There were no significant differences (ANOVA repeated measures) in maximal shortening velocity (~ 280 mm s⁻¹) between the different muscle lengths. The force–velocity curves at the lengths below Lo_{iso} showed that forces at all velocities were higher at $Lo_{iso} - 2$ mm than at $Lo_{iso} - 4$ mm and both were higher than at $Lo_{iso} - 6$ mm. The relation for Lo_{iso} crossed the curve of $Lo_{iso} - 2$ mm between $v = 25$ and 50 mm s⁻¹ and the curve for $Lo_{iso} - 4$ mm around $v = 100$ mm s⁻¹, about the velocity at which power output was maximal for all relative muscle lengths. The highest power output ($P < 0.05$) was found at $Lo_{iso} - 2$ mm (mean \pm s.e.m. 435 ± 19 mW; $n = 8$). Peak power output measured at Lo_{iso} (390 ± 10 mW) and $Lo_{iso} - 4$ mm (395 ± 12 mW) were not significantly different, whereas peak power was lowest ($P < 0.05$) at $Lo_{iso} - 6$ mm (223 ± 15 mW).

There was a significant (Student's paired t test; $P < 0.01$) shift of ~ 1.5 mm in optimum muscle length for force generation during shortening contractions compared with isometric contractions. Shortening velocity had only a relatively small influence on optimum muscle length. It is concluded that fully activated muscles produce their maximal power at a length lower than Lo_{iso} . The difference in optimum length between isometric and dynamic contractions may be a consequence of length-dependent differences in heterogeneity of sarcomere length in series during shortening.

de Haan, A. (1998). *Exp. Physiol.* **83**, 77–84.

All procedures accord with current National guidelines.

Eccentric force–velocity characteristics are similar in oxidative and glycolytic parts of rat medial gastrocnemius muscle

J.M. Rijkkelijkhuizen, C.J. de Ruiter, P.A. Huijting and A. de Haan

Institute for Fundamental and Clinical Human Movement Sciences, Vrije Universiteit, Van der Boechorststraat 9, 1081 BT Amsterdam, The Netherlands

Whereas there is an abundance of data on the effects of muscle fibre type composition on metabolic and contractile properties during isometric and concentric contractions, there is little information regarding the effects during eccentric action. Rat medial gastrocnemius (GM) muscle consists of a proximal part which contains mostly oxidative fibres and a distal part which is dominated by glycolytic fibres. Using selective stimulation of branches of the GM nerve, it has been shown that the distal part generates more power but fatigues faster than the proximal part (de Ruiter *et al.* 1995). Studying fibre type effects on contractile characteristics within the same muscle has the advantage that morphological and mechanical differences are smaller than when two different muscles are compared. The goal of the present study was to investigate whether, similar to shortening contractions, oxidative and glycolytic parts of the GM differ also in their responses to active stretch at different velocities.

In situ experiments were performed on GM muscle–tendon complexes of anaesthetised (urethane, 1.5 g kg⁻¹ i.p.) male Wistar rats ($n = 12$, body mass 243–302 g). Proximal and distal muscle parts (each $n = 6$) were activated maximally. The muscles were subjected to eccentric contractions at eight different velocities (5, 10, 15, 20, 40, 60, 100, 150 mm s⁻¹) in random order. Stretches (3 mm) started from a maximal isometric force plateau (F_{before}) at 2.5 mm below optimum length. After reaching peak eccentric force (F_{peak}), stimulation was continued for 100 ms to obtain isometric force after stretch (F_{after}). Normalised eccentric force was calculated as $(F_{\text{peak}} - [F_{\text{after}} - F_{\text{before}}])/F_{\text{before}}$ (de Ruiter *et al.* 2000) and expressed as a percentage. After the experiments, the animals were humanely killed.

Maximal isometric forces were 5.1 ± 1.7 and 5.4 ± 1.8 N (mean \pm s.d.) for the proximal and distal part ($P > 0.05$, Student's unpaired t test), respectively. There was a significant effect of velocity on eccentric force, with no differences between muscle parts ($P < 0.05$, ANOVA repeated measures). Maximum normalised forces were obtained at 60 mm s⁻¹ and were 157 ± 3 and $153 \pm 6\%$ for the proximal and distal part, respectively. In conclusion, oxidative and glycolytic parts of rat GM have similar eccentric force–velocity relationships despite differences in metabolic, isometric and concentric contractile properties. Apparently, fibre type composition affects muscle function more when muscles are used as a motor than when used as a brake.

de Ruiter, C.J. *et al.* (1995). *Acta Physiol. Scand.* **153**, 313–324.

de Ruiter, C.J. *et al.* (2000). *J. Physiol.* **526**, 671–681.

All procedures accord with current National guidelines.

A calcium-dependent non-cross-bridge stiffness in frog skeletal muscle

B. Colombini, M.A. Bagni, R. Berlinguer Palmmini, P. Geiger and G. Cecchi

Dipartimento di Scienze Fisiologiche, University of Florence, Viale G.B. Morgagni 63, I-50134 Firenze, Italy

Our previous data showed that static stiffness increase following the stimulation both in twitch or tetanic contractions has a time course distinct from that of tension and roughly similar to that of internal calcium concentration. We hypothesized that static stiffness could be attributed to elastic properties of elements of the sarcomere structure whose stiffness increases in a calcium-dependent way. The experiments reported here were made to test the validity of this hypothesis. To investigate the effects of intracellular calcium we measured the static stiffness in single frog muscle fibres under different conditions in which isometric tension was inhibited either by reducing calcium release or by a direct inhibition on the actomyosin interaction.

Frogs (*Rana esculenta*) were killed by decapitation followed by double pithing. Single fibres, dissected from tibialis anterior muscle, were mounted between the lever arms of a force transducer and a moving coil stretcher by means of aluminium clips. Average sarcomere length in a selected segment (1–2 mm long) of the fibre was measured using a striation follower device. The temperature was maintained constant at 14°C. The experiments were made in Ringer and test solutions containing one of the following agents: 2,3-butanedione monoxime (BDM) at 1–5 mM concentration, dantrolene and methoxyverapamil (D600) at 5–10 μ M concentration, deuterium oxide Ringer (98% of water substituted with D₂O) and hypertonic solution up to 1.6 normal tonicity. To measure the static stiffness the fibres were

rapidly stretched (up to 40 nm per half-sarcomere and about 0.5 ms duration) and hold for a period longer than the twitch time course. The fast tension transient was followed by a period during which the tension remained constant at a level that greatly exceeded the isometric force. This level is the static tension and the ratio between the static tension and the accompanying sarcomere length is the static stiffness. The complete time course of static stiffness was determined by applying stretches with different delays with respect to the stimulation.

The results show (Table 1) that static stiffness is almost unaffected by BDM and hypertonic solution, agents that inhibit tension generation mainly by affecting actomyosin interaction reducing cross-bridge formation, even at BDM concentration or Ringer tonicity that reduced twitch tension by more than 90%. In contrast, a similar degree of tension inhibition was accompanied by strong static stiffness reduction when deuterium oxide, dantrolene or D600, agents which mainly reduce the calcium release, were used to inhibit tension generation.

Table 1. Relative values to normal Ringer solution

Tension inhibitors	Concn	Mean relative tension	\pm S.E.M.	Mean relative static stiffness	\pm S.E.M.	n
D600	20 μ M	0.134	0.049	0.248	0.079	4
D ₂ O	98 %	0.081	0.022	0.569	0.066	5
Dantrolene	6.25 μ M	0.202	0.038	0.641	0.038	4
BDM	2.5 mM	0.116	0.007	0.936	0.020	4
Hypertonicity	1.4 T	0.279	0.041	0.977	0.030	5

Our data show that the static stiffness increase in frog skeletal muscle is calcium dependent, in line with our hypothesis, suggesting that the elastic sarcomere structure responsible for static stiffness may be calcium sensitive.

All procedures accord with current National guidelines.

A lesser proportion of fast myosin heavy chain isoforms in older men is closely related to a lower velocity at which peak power occurs during inertial sprint cycling

S.J. Pearson, M.J. Cobbold, R. Orrell* and S.D.R. Harridge

Departments of Physiology and *Neurology, Royal Free and University College Medical School, London, UK

Peak power output and the velocity at which peak power occurs (V_{opt}) during sprint cycling has been shown to be lower in older people (Davies *et al.* 1983). The lower power output can be explained in part by reduced muscle mass; however, this should not explain the lower V_{opt} . It was the aim of the present study to determine if the lower V_{opt} in older people is related to a lower proportion of fast myosin isoforms in their quadriceps muscle.

We examined the power–velocity characteristics of 14 healthy men (7 young, 29 ± 2 years; 7 old, 74 ± 2 years) using a recently developed inertial cycle system (Pearson *et al.* 2002). Prior to testing, a standardised 5 min warm-up was undertaken, two maximal sprints were then performed at five inertial loads, ranging from 0.16 to 0.54 kg m². The best performance was used for analysis. V_{opt} was determined by a third-order polynomial fitting technique. Following local anaesthesia (1% Lignocaine), muscle biopsy samples were obtained from the vastus lateralis muscle using the needle technique and were subsequently analysed for relative MHC isoform composition using gel electrophoresis (SDS-PAGE).

The mean (\pm S.E.M.) peak power, V_{opt} and % MHC-II (MHC-IIA + MHC-IIX) were 847 ± 47 vs. 406 ± 53 Watts, 120 ± 4 vs. 89 ± 6 r.p.m. and 52 ± 7 vs. $25 \pm 7\%$ for the young and older groups, respectively. All measures were shown to be significantly lower in the elderly group when compared with the young ($P < 0.05$, Student's unpaired t test). V_{opt} was found to correlate significantly with the % MHC-II (Fig. 1).

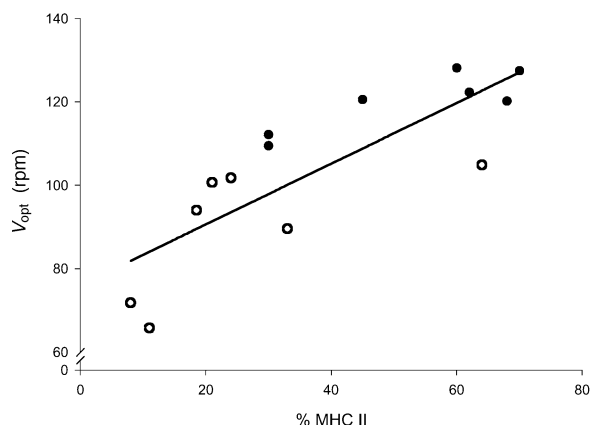


Figure 1. Relationship between %MHC-II and V_{opt} . ●, young; ○, old. $V_{\text{opt}} = 76.9 + 0.72 \text{ MHC-II}$ ($r = 0.82$, $P < 0.001$, $n = 14$).

The results show that the lower V_{opt} in older men relates closely to a lower proportion of the fast contracting MHC-II isoforms in their quadriceps muscle.

Davies, C.T. *et al.* (1983). *Eur. J. Appl. Physiol. Occup. Physiol.* **51**, 37–43.
Pearson, S.J. *et al.* (2002). *J. Physiol.* **539.P**, 59–60P.

S.D.R.H. is a Wellcome Trust Research Fellow.

All procedures accord with current local guidelines and the Declaration of Helsinki.

Nandrolone decanoate treatment affects the steady-state inactivation of contraction and the sarcoplasmic reticulum Ca^{2+} uptake in rat soleus muscle

Aicha Bouhrel, Wissam H. Joumaa and Claude Léoty

Laboratory of General Physiology, CNRS UMR 6018, Nantes University, Faculty of Sciences and Technology, 2 rue de la Houssinière, 44322 Nantes, France

The widespread use and abuse of anabolic androgenic steroids (AAS) have generated tremendous interest in effects, side effects, and raised ethical questions related to the use of these agents, in athletics populations (Shahidi, 2001). However, few studies have been devoted to the analysis at the cellular level of the change due to AAS treatment on the skeletal muscle excitation–contraction coupling mechanism.

Twenty male Wistar rats were divided into two groups; one group received weekly (for 6 weeks) an intramuscular injection of nandrolone decanoate (15 mg kg^{-1}) and the second group received similar doses of vehicle. One week after the last injection, rats were anaesthetised by an ether vapour flow and killed by cervical dislocation; soleus muscle was quickly excised and placed in oxygenated solution. Isolated small bundles (2–4 cells) were dissected for intact and saponin-skinned

experiments and mounted in experimental chambers as already described by Joumaa *et al.* (2002).

In intact fibre bundles, the activation curve of the $[\text{K}^+]_o$ contracture was obtained by a rapid change from the control solution to one containing an elevated potassium concentration (20–146 mM $[\text{K}^+]_o$). The inactivation curve of $[\text{K}^+]_o$ contracture was obtained by measuring test 146 mM $[\text{K}^+]_o$ contracture amplitude after submaximal depolarisation for 2 min in a conditioning $[\text{K}^+]_o$. In this solution, the $[\text{K}^+][\text{Cl}^-]$ product was kept constant to allow rapid recovery of resting membrane potential and restoration of the amplitude of tension response. Membrane potentials were measured in the usual way (Joumaa *et al.* 2002). No significant change was observed in 146 mM $[\text{K}^+]_o$ contracture characteristics after drug treatment (amplitude normalised to saponin-maximal tension: control, $85.7 \pm 2.9\%$; treated, $91.9 \pm 3.1\%$; time-to-peak: control, 13.5 ± 0.5 s; treated, 12.9 ± 0.6 s; time constant of relaxation: control, 5.5 ± 0.3 s, treated, 6.1 ± 0.5 s; $n = 12$, mean \pm S.E.M., ANOVA one-way statistical test). In treated muscle, a shift to more negative potential of the steady-state inactivation curve was found (membrane potential for 50% of inactivation (mV): control, -40.5 ± 1.1 ; treated, -48.7 ± 1.2 ; $n = 10$; $P < 0.05$), whereas no significant change was detected on the voltage dependence activation curve (membrane potential for 50% of activation (mV): control, -38.7 ± 0.4 ; treated, -38.1 ± 0.6 , $n = 10$).

In saponin-skinned fibres, the amount of Ca^{2+} taken up at different loading times in pCa 7.0 solution was estimated by using the amplitude of the contracture due to caffeine application (10 mM). The semilogarithmic plot of the relative tension against time during the different loading time allows estimation of the rate of the Ca^{2+} uptake by the sarcoplasmic reticulum. The loading rate was significantly decreased after 6 weeks of nandrolone decanoate treatment (control: $0.0079 \pm 0.0012 \text{ s}^{-1}$; treated: $0.0039 \pm 0.0007 \text{ s}^{-1}$, $n = 8$, $P < 0.05$).

It has been shown previously that, in frog muscle (Même & Léoty, 1999), the decay of tension in skeletal muscle during prolonged steady-state depolarisation depends not only on inactivation of the process regulating Ca^{2+} release from the sarcoplasmic reticulum, but also on the ability of the sarcoplasmic reticulum to pump Ca^{2+} . Then, in the absence of a significant difference in the relaxation phase of $[\text{K}^+]_o$ contracture between treated and control soleus fibres, it could be proposed that, in treated muscle, the effect of the shift in the steady-state inactivation curve was compensated for by the slowing of Ca^{2+} uptake by the sarcoplasmic reticulum.

Joumaa, W.H. *et al.* (2002). *J. Pharmacol. Exp. Ther.* **300**, 638–646.

Même, W. & Léoty, C. (1999). *Acta Physiol. Scand.* **166**, 209–216.

Shahidi, N.T. (2001). *Clin. Ther.* **23**, 1355–1390.

All procedures accord with current National guidelines.

Stimulation of sarcoplasmic reticulum Ca^{2+} -ATPase by disulfiram induces changes in voltage activation of contraction in rat slow-twitch skeletal muscle

Wissam H. Joumaa, Aicha Bouhrel and Claude Léoty

Laboratory of General Physiology, CNRS UMR 6018, Nantes University, Faculty of Sciences and Technology, 2 rue de la Houssinière, BP 92 208, 44322 Nantes, France

In skeletal muscle fibres, potassium contractures have been widely used as a convenient experimental model for the study of depolarisation–contraction coupling. It is generally recognised

that the voltage dependence of tension during steady-state depolarisation depends on activation of the voltage sensor in transverse tubule membrane. Moreover, the slow decay in tension during prolonged depolarisation is assumed to depend exclusively on inactivation of excitation-contraction coupling (Dulhunty, 1991). Disulfiram was found to stimulate the sarcoplasmic reticulum Ca^{2+} -ATPase activity of skeletal muscle (Starling *et al.* 1996). Thus the aim of the present study was to use disulfiram to estimate the role of Ca^{2+} uptake by the sarcoplasmic reticulum on the activation and inactivation of steady-state tension in mammalian slow-twitch muscle.

The experiments were performed at 19–20°C on soleus small bundles (2–4 cells) isolated from adult male Wistar rats anaesthetised by an ether vapour flow and then killed by cervical dislocation. Preparations were mounted in the experimental chamber as described by Joumaa *et al.* (2002). The application of an elevated potassium concentration (20–146 mM $[\text{K}^+]_o$) allowed us to obtain the activation curve, and the inactivation curve of $[\text{K}^+]_o$ contracture was obtained by measuring test 146 mM $[\text{K}^+]_o$ contracture amplitude after submaximal depolarisation for 2 min in a conditioning $[\text{K}^+]_o$. In this solution, the $[\text{K}^+][\text{Cl}^-]$ product was kept constant to allow rapid recovery of resting membrane potential and restoration of the amplitude of tension response. Membrane potentials were measured in the usual way (Joumaa *et al.* 2002). The values of membrane potential for half-maximal activation (E_a) and inactivation (E_i) of contraction were obtained by fitting the Boltzman equation for each fibre in the experiment.

Disulfiram (3.1–62.5 μM) reversibly reduced the amplitude (control: 1.5 ± 0.3 mN, 27 μM disulfiram: 1.0 ± 0.1 mN, $n = 12$, $P < 0.05$, mean \pm S.E.M., Student's paired t test), the time to peak tension (control: 14.1 ± 0.5 s, 27 μM disulfiram: 9.8 ± 0.8 s, $n = 12$, $P < 0.05$) and the time constant of relaxation (control: 8.5 ± 0.2 s, 27 μM disulfiram: 5.9 ± 0.3 s, $n = 12$, $P < 0.05$) of 146 mM $[\text{K}^+]_o$ contracture. In the presence of 27 μM disulfiram, the relationship between the amplitude of potassium contractures and the membrane potential was shifted to less negative potentials (control: $E_a = -43.5 \pm 1.1$ mV, disulfiram: $E_a = -29.7 \pm 2.3$ mV, $n = 8$, $P < 0.05$), whereas the steady-state inactivation curve was unchanged (control: $E_i = -39.9 \pm 0.6$ mV, disulfiram: $E_i = -38.6 \pm 1.7$ mV, $n = 8$, $P < 0.05$), suggesting that disulfiram has no effect on voltage sensor. The difference presently found between potassium contractures in the absence and presence of disulfiram implies that, as previously reported in frog muscle (Même & Léoty 1999), the peak amplitude and the slow relaxation of tension during prolonged steady-state depolarisation depends not only on inactivation of the process regulating Ca^{2+} release from the sarcoplasmic reticulum, but also on the ability of the sarcoplasmic reticulum to pump Ca^{2+} .

Dulhunty, A.F. (1991). *J. Physiol.* **439**, 605–626.

Joumaa, W.H. *et al.* (2002). *J. Pharmacol. Exp. Ther.* **300**, 638–646.

Même, W. & Léoty, C. (1999). *Acta Physiol. Scand.* **166**, 209–216.

Starling, A.P. *et al.* (1996). *Biochemistry* **320**, 101–105.

All procedures accord with current National guidelines.

Sarcomere length–tension relationship during slow shortening of fully and partially activated intact fibres of frog skeletal muscle

L. Pizza and A. Scialp

Dipartimento di Scienze Fisiologiche, Università di Firenze, Viale G.B. Morgagni 63, I-50134 Firenze, Italy

Our previous results (Colomo *et al.* 1998) showed that the optimal sarcomere length (SL) for force development in intact muscle fibres, activated with submaximal contractures, shifted to a sarcomere length longer than would be expected on the basis of myofilament overlap. These results, obtained under 'fixed-end' conditions are consistent with the evidence obtained in skinned fibres showing that the optimal SL for force development shifted at larger values when the $[\text{Ca}^{2+}]$ in the myoplasm was lowered. It could be objected, however, that because of a possible non-homogeneous activation, even in submaximal contractures significant fibre portions could still be at full or near full activation. If this were the case the tension creep generated by these fully activated portions could be responsible, at least partially, for the increase in tension observed at long SL. To clarify this point we determined the length–tension relationship under isometric conditions and during slow fibre shortening (shortening velocity was 10–15% of maximum velocity), a condition which has been shown to eliminate the tension creep (Morgan *et al.* 1991). Single fibres, isolated from the interosseus digiti IV muscle of *Rana esculenta* (frogs were killed by decapitation followed by double pithing), were mounted between a force transducer and a length-control motor. Experiments were made in 'fixed-end' conditions at SL between 2.10 and 3.10 μm , at a temperature of 18°C. SL was measured directly by a laser diffractometer, or was calculated from fibre length. The shape of the isometric length–tension relationship in both maximum tetani or maximal contractures ($[\text{K}^+]_o = 190$ mM), was similar to that already described in the literature for 'fixed-end' conditions. In contrast, when the tension was measured during shortening, the length–tension relationship had the shape expected on the basis of filament overlap extrapolating to zero at 3.55 μm SL. In submaximal contractures ($[\text{K}^+]_o = 30$ –48 mM, and isometric tension of 0.2–0.4 P_0), in both isometric and shortening conditions, the ascending limb of the length–tension relationship had a similar shape: it increased with sarcomere length reaching a peak at 2.80–3.00 μm . In both conditions the maximum peak tension corresponded to the value expected on the basis of filament overlap. This result shows that the shape of the isometric length–tension relationship, in our experiments with submaximal contractures, is not affected by tension creep. We conclude that: (i) submaximal contracture is a suitable model to obtain, in intact fibres, conditions of partial and homogeneous activation (low internal Ca^{2+}); (ii) the increase in apparent sensitivity of tension to $[\text{Ca}^{2+}]_i$ that occurs in skinned fibres at long SL also occurs in intact fibres.

Colomo, F. *et al.* (1998). *J. Mus. Res. Cell Motil.* **19**, 303.

Morgan, D.L. *et al.* (1991). *J. Physiol.* **441**, 719–732.

All procedures accord with current National guidelines.